Spin Multiplicity and Symmetry Breaking in Vanadium-Benzene Complexes

L. Horváthová,[1] M. Dubecký,[1] L. Mitas,[2] and I. Štich[1,*]

[1]*Institute of Physics, CCMS, Slovak Academy of Sciences, 84511 Bratislava, Slovakia*
[2]*Department of Physics and CHiPS, North Carolina State University, Raleigh, North Carolina 27695, USA*
(Received 21 November 2011; published 31 July 2012)

We present accurate quantum Monte Carlo (QMC) calculations which enabled us to determine the structure, spin multiplicity, ionization energy, dissociation energy, and spin-dependent electronic gaps of the vanadium-benzene system. From total and ionization energy we deduce a high-spin state with vastly different energy gaps for the two spin channels. For this purpose we have used a multistage combination of techniques with consecutive elimination of systematic biases except for the fixed-node approximation in QMC calculations. Our results significantly differ from the established picture based on previous less accurate calculations and point out the importance of high-level many-body methods for predictive calculations of similar transition metal-based organometallic systems.

Complexes of $3d$ transition metal atoms (TM) with benzene molecule(s) (Bz), TMBz, represent one of the most important families of π-bonded organometallics [1]. In the gas phase, these systems can be produced either by conventional synthetic procedures or by laser vaporization techniques [2,3]. Mass spectra experiments [4] of $TM_n^+Bz_m$ complexes indicate presence of two types of atomic structures: (i) rice-ball structures, with either several atoms coating the benzene or with benzene molecules wrapped around one or a few TM atoms and (ii) the sandwich-type structures $TM_n^+Bz_{n+1}$, with the basic building block being the half-sandwich TMBz, see Fig. 1. The sandwich structures are of particular interest since they can exhibit ferromagnetic-antiferromagnetic coupling [5,6] and therefore energy differences of the order of chemical accuracy (≈ 1 mHa or 0.04 eV) are of paramount importance. Their properties are expected to vary across the TM series, with the early and late TMBz systems showing distinctly different properties [7,8]. In addition, previous studies have revealed a wealth of interesting magnetic [8–10] and transport effects [5,11]. Among the most important and intriguing applications is the use of sandwich-type TM-benzenes as spin valves, featuring system-size dependent metallic behavior for the majority spin electrons and a semiconductor gap for the minority spin electrons [11]. The applicability potential is enhanced by the possibility of stacking such units into longer chains with tunable properties for spintronics applications.

In order to shed new light on this family of systems, we have performed a case study of one particular member, namely VBz half-sandwich and, using QMC methods, we predict a completely new picture for its properties. Using the explicitly correlated QMC techniques, we clearly demonstrate that the questions related to the spin multiplicities and associated effects in TMBz(s) are much too subtle for more approximate mainstream methods and that top accuracy many-body approaches are crucial to provide both predictive power and consistent comparison with experiments.

Our Letter seeks to answer three primary questions: (1) what happens to a transition metal atom with unpaired $3d$ electrons when anchored on an organic molecule such as benzene; (2) what is the TMBz bonding strength resulting from such interactions; and (3) what are the corresponding spin gaps for majority and minority spin channels. In particular, will the vanadium outer electrons seek to maximize the spin multiplicity to six even when bonded to benzene or the opposite will happen and the spin of the vanadium atom will be quenched?

To the best of our knowledge, so far only density-functional theory (DFT) techniques have been applied to answer the above questions [5,6,8–10]. The earlier studies suggested that magnetic moments or spin multiplicities of transition metal atoms embedded in TMBz complexes were increasing from Sc to Cr and decreasing from Mn
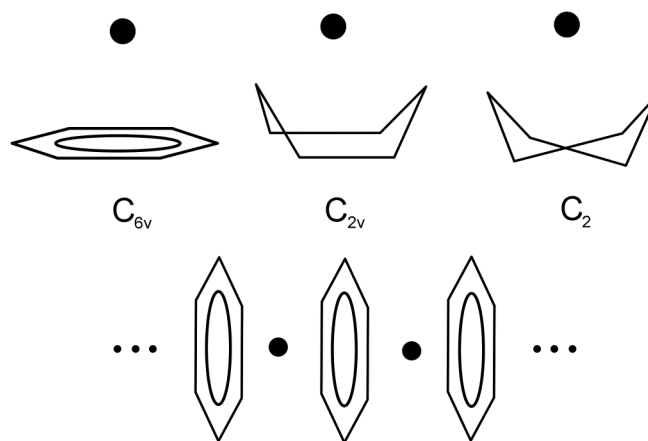

FIG. 1. Half-sandwich (top panel) and sandwich-type (lower panel) of structures of TMBz complexes. Schematics of possible Jahn-Teller distortions are shown in the top panel.

to Ni in analogy with their behavior when supported on metal surfaces [8,12]. However, the robustness and reliability of these DFT predictions have been undermined by later studies which found conflicting results for spin multiplicities and dissociation energies pointing thus to a limited accuracy of DFT for these important quantities. Despite the keen interest in these systems, experiments alone do not provide enough insights either. The experiments deal almost exclusively with cations and information on the neutral TMBz complexes, for instance dissociation energies, are usually determined indirectly from measured dissociation energies on cations, which themselves exhibit large spread due to experimental bias [13–15].

Having in mind the limitations of previous studies we have performed the most accurate and complete study of vanadium-benzene half-sandwiches using the advanced correlated QMC method [16]. QMC calculations offer a favorable scaling with the system size and its accuracy is limited only by the choice of the nodal hypersurface of the many-body wave function [16]. In addition, the sensitivity of the key geometry parameters prompted us to apply QMC calculations to structural optimizations as well, making thus another step beyond mainstream QMC studies. We deal with both these challenges by first determining sufficiently accurate nodal hypersurfaces followed by QMC structural optimization which eliminates possible bias coming from geometries determined solely in less accurate methods such as DFT. This iterated QMC strategy then enables us to determine the structure, spin multiplicity, ionization energy, dissociation energy, and spin-dependent electronic gaps of the VBz system. For the VBz system we find ground-state spin multiplicity and dissociation energy that differ significantly from the previous DFT results. At the same time, our study points towards shortcomings and possible biases in the existing experimental results.

All simulations used the following five-level refinement strategy which enabled us to filter out basically all of the systematic biases: (1) initial geometries were obtained from DFT optimization, (2) trial wave function was constructed using a DFT nodal hypersurface, (3) trial wave function was optimized using VMC (variational Monte Carlo) techniques, (4) energies were computed from DMC (diffusion Monte Carlo) simulations, and (5) geometry was optimized at the QMC level with focus on the key V-Bz distance. For static DFT and complete-active-space self-consistent-field method (CASSCF), we used the GAMESS suite of codes [17], while all VMC and DMC calculations used the QWALK code [18].

The ground-state geometries were initially calculated using DFT techniques with generalized gradient approximation-type (GGA) Becke-Perdew-Wang 91 (BPW91) [19,20], hybrid Becke-three-parameter-Lee-Yang-Parr (B3LYP) [21], meta-hybrid Tao-Perdew-Staroverov-Scuseria (TPSSh) [22], and double-hybrid Becke-two-parameter-Lee-Yang-Parr (B2PLYP) [23] exchange-correlation (xc) functionals. These

xc-functionals, except for B2PLYP where construction of the wave function is more intricate, were also used in the DFT energy calculations and in construction of trial wave functions for the fixed-node QMC calculations. Use of the BPW91 functional was motivated mainly by comparison purposes since previous DFT studies of VBz employed either the BPW91 functional [8–10] or the related PBE functional [6,24]. The impact of exact exchange mixing and kinetic energy density or MP2 correlation can be judged from comparison between B3LYP, TPSSh, B2PLYP, and BPW91 results. The Greeff-Lester type (nonsingular) effective core pseudopotential [25,26] and correlation-consistent polarized valence-only triple zeta basis sets [27] were used for all species. We have tested various active spaces in the CASSCF method to determine the impact of correlation on the orbitals and corresponding nodal hypersurfaces for the V^+, V, Bz, VBz^+, and VBz complexes. While there was little difference in the atom and Bz case, in the VBz/VBz^+ complexes the nodal hypersurfaces constructed from the CASSCF orbitals provided inferior accuracy to those obtained from the (mean-field correlated) DFT orbitals [28]. The Jastrow factors of the Schmidt-Moskowitz type [29] have included electron-electron, electron-nucleus, and electron-electron-nucleus correlations. In the course of DFT geometry optimizations we found that V-Bz distance is the least robustly determined structural degree-of-freedom. Therefore the V-Bz distance was QMC-reoptimized using simple parabolic fits.

We have considered three multiplicities of VBz, namely 2, 4, and 6. Our DFT optimized energies for both functionals are summarized in Fig. 2 and Tab. I. The system exhibits spin multiplicity-dependent atomic structure. Using symmetry unconstrained optimization we found that for $M = 2$ the system adopts C_{2v}/C_6 symmetry, depending on the xc-functional used. For $M = 4$ the system lowers the energy by lowering the symmetry to C_1 which,
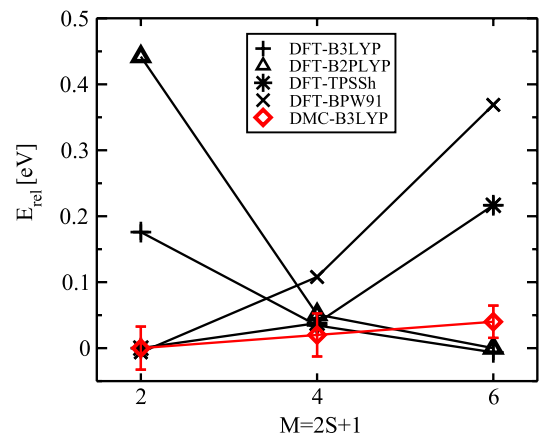

FIG. 2 (color online). Energies, relative to the minimum, of VBz for various spin multiplicities calculated in the DFT and DMC/B3LYP approaches.

TABLE I. QMC energies of VBz for spin multiplicities $M = 2, 4, 6$ after QMC optimization of the V-Bz distance, see Fig. 3. r is the average distance between V and benzene C atoms.

M	Trial w.f.	Symmetry	E_{DMC} a.u.	E_{rel}^{DMC} eV	r Å
	TPSSh	C_6	$-108.9296(8)$	0.00(4)	2.10
2	B3LYP	C_{2v}	$-108.9254(12)$	0.10(4)	2.09
	BPW91	C_{2v}	$-108.9243(10)$	0.13(4)	2.10
	TPSSh	C_1	$-108.9259(7)$	0.08(4)	2.23
4	B3LYP	C_1/C_2	$-108.9248(7)$	0.12(5)	2.21
	BPW91	C_1	$-108.9243(7)$	0.13(4)	2.23
	TPSSh	C_1	$-108.9250(7)$	0.11(4)	2.43
6	B3LYP	C_1	$-108.9241(9)$	0.14(4)	2.45
	BPW91	C_1	$-108.9199(10)$	0.25(4)	2.43

in practical terms, is very similar to the zigzag C_2 geometry, see Fig. 1. For $M = 6$ the symmetry is reduced to C_1, irrespective of the xc-functional used. Such a structure results in a "wavy" configuration of Bz with the V atom moving away from the center of the Bz ring. The symmetry reduction, while small in geometrical terms, reduces the DFT energies by up to ≈ 0.2 eV. The increase of the spin multiplicity is accompanied by a systematic increase in the medium V-C distance from ≈ 2.10 Å for $M = 2$, to ≈ 2.45 Å for $M = 6$. The DFT calculations lead to contradictory results for the ground-state spin multiplicities, with B3LYP and B2PLYP predicting VBz to be spin sextet, whereas BPW91 and TPSSh favor the spin doublet, see Fig. 2. The energy margins for both multiplicities are of the order of ≈ 0.5 eV. Hence, particular choice of the xc-functional affects the DFT energies by a factor exceeding chemical accuracy by an order of magnitude and leads to opposite prediction of the stable spin multiplets.

The fixed-node DMC/BPW91, DMC/B3LYP, and DMC/TPSSh calculations, Tab. I, at optimized geometries find qualitatively very similar results for $M = 2, 4,$ and 6 multiplicities yielding nearly degenerate energies within the margin of ≈ 0.1 eV. From all these results we conclude that use of DFT nodal hypersurfaces introduces an uncertainty of the order of 0.1 eV. We note in passing that DMC compresses the energy scale from the DFT scale of ≈ 0.5 eV to ≈ 0.1 eV, hence by a factor of 5. This makes us to conclude that all nodal hypersurfaces yield essentially degenerate energies. Based on total energy only, given the (≈ 0.1 eV) DMC error bars it is impossible to decide spin multiplicity of VBz directly even with the QMC methods.

In order to discriminate between the different almost degenerate spin states we calculate the vertical ionization potentials (IP) for each multiplicity. The result is listed in Tab. II along with the summary of calculated dissociation energies E^D and comparison with experimental values and other calculations. We conclude that only the DMC IP calculated in $M = 6$ multiplicity is in good agreement with the experimental value. The DFT IPs are reasonably

TABLE II. Dissociation/vertical ionization energy of VBz in eV. E_{DFT}^D labels DFT dissociation energies, E_{DMC}^D/IP$_{DMC}$ the DMC dissociation/ionization energy. E_{exp}^D/IP$_{exp}$ are the experimental dissociation/vertical ionization energy.

M	Trial w.f.	E_{DFT}^D	E_{DMC}^D	E_{exp}^D	IP$_{DMC}$	IP$_{exp}$
2		1.57	0.77(3)		5.69(3)	
4	TPSSh	1.53	0.67(3)		5.26(4)	
6		1.35	0.64(3)		5.01(3)	
2		0.17	0.65(5)		5.61(4)	
4	B3LYP	0.31	0.63(5)	0.78(9)[c]	5.37(3)	
6		0.35	0.61(5)	0.74(9)[d]	5.01(4)	5.11(4)[f]
2		1.92	0.65(4)	1.05(21)[e]	5.61(4)	
4	BPW91	1.80	0.65(4)		5.37(3)	
6		1.54	0.53(4)		4.94(4)	
2[a]		2.09	-		5.71	
4[a]	BPW91	0.67	-		5.53	
6[b]		0.81	-		5.27	

[a]Reference [10].
[b]References [8,9].
[c]Reference [13].
[d]Reference [14].
[e]Reference [15].
[f]Reference [4].

close to the experimental value of 5.11(4) eV and of comparable quality to the DMC results. However, this is clearly an effect of error cancellation, since similar underbinding (B3LYP, B2PLYP) or overbinding (BPW91, TPSSh) biases affect both the cation and the neutral VBz. All other multiplicities yield significantly worse agreement with the experiment. Hence, we conclude that the most probable spin multiplicity is the spin sextet. This conclusion is also in agreement with the high spin-state of the cation [28,30]. Comparison based on IP is a very stringent test as the vertical ionization energies are experimentally directly measurable.

Contrary to the ionization energies, dissociation energies are experimentally estimated only indirectly using the relation [8–10] $E_D(TMBz) = E_D(TMBz^+) + IP(TMBz) - IP(TM)$, where $E_D(TMBz^+)$ is dissociation energy of the cationic TMBz, and IP(TMBz) and IP(TM) are vertical ionization potentials of TMBz and TM atom, respectively. Such a formula would only be strictly valid if adiabatic ionization potentials were used. Computationally the dissociation energies are calculated directly. They require knowledge of the fragments, the atom and the Bz molecule. While Bz molecule is easy to compute accurately, it is somewhat more complicated to calculate the energy of the ^4F $(3d^3 4s^2)$ ground-state of the V atom accurately since the wave function requires two determinants to describe correctly the spatial-spin symmetries. At the DMC level, we obtain for the ionization process ($^4F \rightarrow ^5D$) 6.64(2) eV [28] compared to the experimental 6.75 eV [31]. We find quite staggering dissociation energy differences between the different DFT functionals. For example, for the doublet
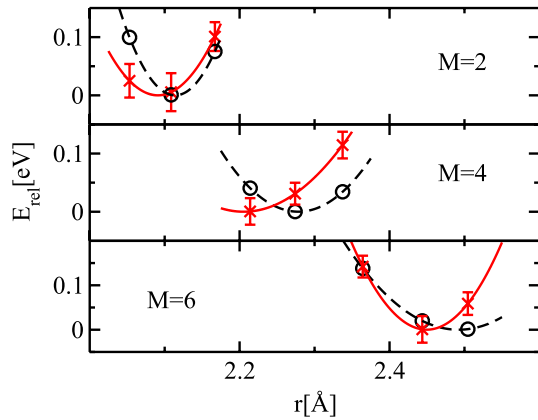
FIG. 3 (color online). Energies, aligned to zero, of VBz for $M = 2, 4, 6, 4, 6$ as a function of the average V-C distance r in DFT-B3LYP (dashed line) and DMC/B3LYP (points with error bars and fit/full line) approaches.

state B3LYP yields 0.17 eV, B2PLYP renders it unstable (not shown), while TPSSh yields 1.57 eV and BPW91 1.92 eV. However, our DFT calculations do not reproduce the previous DFT studies [8–10] which find dissociation energies between 0.67 and 2.09 eV for the three spin multiplicities, Tab. II, even if we use the same xc-potential. These differences arise most likely due to a combination of smaller basis sets and use of high-symmetry structures in the previous studies. Surprisingly, even multireference configuration-interaction calculation (CI) method (with the largest virtual space that could be afforded) finds negligible bonding energy of 0.03 eV and $M = 4$ [32] in complete disagreement with the experiment and all other theoretical estimates. Our DMC dissociation energies of ≈ 0.65 eV turn out to be very robust and only weakly dependent on the xc-functional used to construct the nodal hypersurfaces. Experiments yield dissociation energies between 0.74 and 1.05 eV. Note, however, that these values are obtained only indirectly using possibly shifted dissociation energy of the cation [13–15] and the vertical ionization energy instead of the adiabatic one. Taking into account these considerations, our DMC values all fall within the large experimental error bars which include mentioned systematic biases.

Motivated by the intentions of using TMBz sandwiches as spin valves, we have calculated the corresponding gaps for the VBz half-sandwich. While in DFT methods this is often calculated as highest occupied molecular orbital-lowest unoccupied molecular orbital (HOMO-LUMO) gap, in the many-body QMC, the calculations of the gap are obtained as differences of total energies [16] as given by $E_g^{\uparrow,\downarrow} = (E_{N+1}^{\uparrow,\downarrow} - E_N) - (E_N - E_{N-1}^{\uparrow,\downarrow})$. At the DMC level we find $E_g^{\uparrow} = 4.90$ eV and $E_g^{\downarrow} = 10.04$ eV compared to HOMO-LUMO $E_g^{\uparrow} = 2.34$ eV and $E_g^{\downarrow} = 6.28$ eV from DFT, about a factor of two smaller. The difference between the spin-majority and spin-minority gaps is expected to increase with the sandwich length [11].

In summary, we have carried out study of the vanadium-benzene organometallic complex using the explicitly correlated QMC methods. These calculations also involved QMC geometry optimizations and a multistage strategy to eliminate basically all systematic biases except the fixed-node error. Although the QMC calculations are much more demanding computationally, the results enabled us to shed new light on the previous DFT calculations and their inconsistencies as well as to reveal genuine DFT biases. For example, we found incorrect and varying energy ordering of spin multiplets depending on the employed functional. The errors are of the order of few tenths of eV, which is very significant considering the true spin-flip energies. Interestingly, QMC results suggest that the available states are basically degenerate. Furthermore, we were able to consistently identify the states of interest in theory and experiment using accurate values of ionization energies. Our calculations also yielded dissociation energies which point out the possible presence of biases in corresponding experimental values, and we calculated spin gaps which are of interest for spintronics applications. These calculations not only offer new insights for VBz systems but also open new opportunities for using QMC methods for many other organometallic systems of similar importance.

---

*ivan.stich@savba.sk

[1] D. Braga, P. J. Dyson, F. Grepioni, and B. F. G. Johnson, Chem. Rev. **94**, 1585 (1994).

[2] J. C. Ma and D. A. Dougherty, Chem. Rev. **97**, 1303 (1997).

[3] D. A. Dougherty, Science **271**, 163 (1996).

[4] T. Kurikawa, H. Takeda, M. Hirano, K. Judai, T. Arita, S. Nagao, A. Nakajima, and K. Kaya, Organometallics **18**, 1430 (1999).

[5] H. Xiang, J. Yang, J. G. Hou, and Q. Zhu, J. Am. Chem. Soc. **128**, 2310 (2006).

[6] Y. Mokrousov, N. Atodiresei, G. Bihlmayer, S. Heinze, and S. Blügel, Nanotechnology **18**, 495402 (2007).

[7] M. A. Duncan, Int. J. Mass Spectrom. **272**, 99 (2008).

[8] R. Pandey, B. K. Rao, P. Jena, and J. M. Newsam, Chem. Phys. Lett. **321**, 142 (2000).

[9] R. Pandey, B. K. Rao, P. Jena, and M. A. Blanco, J. Am. Chem. Soc. **123**, 3799 (2001).

[10] A. K. Kandalam, B. K. Rao, P. Jena, and R. Pandey, J. Chem. Phys. **120**, 10414 (2004).

[11] V. V. Maslyuk, A. Bagrets, V. Meded, A. Arnold, F. Evers, M. Brandbyge, T. Bredow, and I. Mertig, Phys. Rev. Lett. **97**, 097201 (2006).

[12] K. Wildberger, V. S. Stepanyuk, P. Lang, R. Zeller, and P. H. Dederichs, Phys. Rev. Lett. **75**, 509 (1995).

[13] F. Meyer, F. A. Khan, and P. B. Armentrout, J. Am. Chem. Soc. **117**, 9740 (1995).

[14] C.-N. Yang and S. J. Klippenstein, J. Phys. Chem. A **103**, 1094 (1999).

[15] R. L. Hettich, T. C. Jackson, E. M. Stanko, and B. S. Freiser, J. Am. Chem. Soc. **108**, 5086 (1986).

[16] W. M. C. Foulkes, L. Mitas, R. J. Needs, and G. Rajagopal, Rev. Mod. Phys. **73**, 33 (2001).

[17] M. W. Schmidt *et al.*, J. Comput. Chem. **14**, 1347 (1993).

[18] L. Wagner, M. Bajdich, and L. Mitas, J. Comput. Phys. **228**, 3390 (2009).

[19] A. D. Becke, Phys. Rev. A **38**, 3098 (1988).

[20] J. P. Perdew and Y. Wang, Phys. Rev. B **45**, 13244 (1992).

[21] A. D. Becke, J. Chem. Phys. **98**, 5648 (1993).

[22] V. N. Staroverov, G. N. Scuseria, J. Tao, and J. P. Perdew, J. Chem. Phys. **119**, 12129 (2003).

[23] T. Schwabe and S. Grimme, Phys. Chem. Chem. Phys. **9**, 3397 (2007).

[24] J. P. Perdew, K. Burke, and M. Ernzerhof, Phys. Rev. Lett. **77**, 3865 (1996); Phys. Rev. Lett. **78**, 1396 (1997).

[25] C. W. Greeff and W. A. Lester, J. Chem. Phys. **109**, 1607 (1998).

[26] I. Ovcharenko, A. Aspuru-Guzik, and W. A. Lester, J. Chem. Phys. **114**, 7790 (2001).

[27] T. H. Dunning, Jr, J. Chem. Phys. **90**, 1007 (1989).

[28] L. Horváthová, M. Dubecký, L. Mitas, and I. Štich (to be published).

[29] K. E. Schmidt and J. W. Moskowitz, J. Chem. Phys. **93**, 4172 (1990).

[30] P. M. Polestshuk, P. I. Dem'yanov, and I. G. Ryabinkin, J. Chem. Phys. **129**, 054307 (2008).

[31] Y. Osanai, H. Ishikawa, N. Miura, and T. Noro, Theor. Chem. Acc. **105**, 437 (2001).

[32] F. Rabilloud, J. Chem. Phys. **122**, 134303 (2005).